Neutron Physics

MIT Department of Physics
(Dated: October 16, 2014)

The technique of time-of-flight spectroscopy with a mechanical beam chopper is used to study the properties of thermal neutrons in a beam emerging from the MIT Research Reactor (MITR-II) at the MIT Nuclear Reactor Laboratory. First, the distribution in velocity of the neutrons is measured, and the results are compared with the Maxwell-Boltzmann distribution for the temperature of the reactor. Second, the De Broglie relation between wavelength and momentum of neutrons is determined from measurements of the angle of Bragg reflection of the beam from a copper crystal as a function of the velocity measured by time-of-flight. Third, the absorption cross sections of several elements are measured, and the $1/v$ dependence of the boron cross section is observed.

PREPARATORY QUESTIONS

Please visit the Neutron Physics chapter on the 8.13x website at mitx.mit.edu to review the background material for this experiment. Answer all questions found in the chapter. Work out the solutions in your laboratory notebook; submit your answers on the web site.

SAFETY

Training Requirements

The following must be completed *before* starting the experiment:

1. Peruse the MIT NRL website and familiarize yourself with the reactor setup and experimental facilities: http://web.mit.edu/nrl/www/index.html.

2. Read through the *Neutron Spectrometer Operations Manual*, which is posted in the *Materials* section of the course's Stellar website. Note, this document is protected for class-only access, and should not be shared outside MIT.

3. Radiation Safety: Reactor training (web-based, EHS00311w). This may take up to two hours, and can be done from any computer with MIT personal certificates installed. Instructions can be found in the *Neutron Spectrometer Operation Manual.*

Experimentation at the MIT Research Reactor: Radiation Protection, Access, and Security

As with all nuclear reactor facilities in the United States, access to the reactor building is restricted in accordance with federal regulations administered by the US Nuclear Regulatory Commission. You will be required to complete radiation safety training and be escorted at all times.

In keeping with the spirit of the Junior Lab, you will operate all the equipment yourself during the first lab session at the reactor. After that, you will be able to run the experiment remotely from Junior Lab. Any time you need to visit the experiment in the reactor containment building, you must be escorted by an authorized Junior Lab staff member or NRL personnel. **NRL protocols require that you wear long pants and closed-toe shoes without pointed heels whenever visiting the facility.**

For the purpose of Junior Laboratory experimentation, the following steps should be taken in order to have access to the reactor:

1. First, complete the trainings described in the *Neutron Spectrometer Operation Manual.*

2. Entry into the NRL building is through a locked door on Albany Street which may be opened with an authorized MIT ID, or by ringing the doorbell.

3. Entry procedures for the reactor containment building will be described during the practicum tour. All access to the containment building and the experiment is restricted. You must be accompanied by an authorized escort.

4. For your first scheduled lab period, begin by meeting your lab partner at Junior Lab. An instructor or technical staff member will then take you to the NRL and show you the apparatus and procedures. Please contact Junior Lab staff (extensions x3-5082 or x2-2122) in advance if a conflict or change of schedule interferes with this important introductory session.

5. The equipment is reserved for your use at the scheduled lab time. To operate the experiment remotely you must remotely access the experiment computer. Instructions can be found in the *Neutron Spectrometer Operation Manual.* You should request any proposed changes to your scheduled attendance with your section instructor.

SUGGESTED SCHEDULE

By the end of the second session, you should calculate the velocity of the particles to zeroth order using MCS

distributions of neutron time of flights at the near and far detector positions.
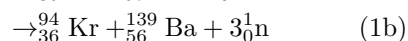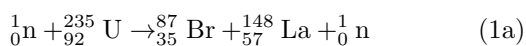
I.   INTRODUCTION

This experiment was developed for Junior Lab by Professor Clifford Shull [1]. It employs a rather intense beam of low energy neutrons produced at the MIT Research Reactor (MITR-II) located in Building NW12 on the edge of the campus at 138 Albany Street. The MIT reactor has been operating since 1958 and has served as a base for countless investigations by faculty, graduate and undergraduate thesis students, UROP and other undergraduate student projects. Use of its facilities is perfectly safe, providing reasonable and common-sense guidelines and procedures are followed. These guidelines and procedures are covered in the training you are instructed to complete in the *Neutron Spectrometer Operation Manual.*

The three main parts of the experiment are: the Maxwell-Boltzmann distribution, Bragg scattering of thermalized neutrons and the De Broglie relation, and finally neutron absorption cross sections.

I.1.   Operational Physics of a Nuclear Reactor

The nuclear reactor is a chain-reacting system which bears resemblance in operational principle to a coal fire, with nuclear reactions being the source of heat rather than chemical reactions. In a coal fire, some carbon atoms are excited by thermal "starting" so that they combine with oxygen (burn). The heat released in this exothermic chemical reaction activates other carbon atoms to do the same, thereby forming a chain reaction without further need of starting. The fire grows in intensity until an equilibrium level is reached, wherein heat losses from the system limit the thermal power available for further steps in the chain reacting process.

In a nuclear reactor, the counterpart to the carbon fuel is the nuclear fuel (most commonly the fissionable isotope of uranium, $^{235}_{92}$U), and neutrons serve as the communicative thermal energy counterpart. In 1939 Hahn and Strassman discovered that neutrons react with uranium nuclei to cause fission in which the heavy nucleus splits into two smaller and not necessarily equal nuclei plus "debris" such as neutrons, gamma-rays, electrons, etc. The fragmentation can proceed in many different ways. Typical reactions are shown in Equation 1.

$$^1_0\text{n} + ^{235}_{92}\text{U} \rightarrow ^{87}_{35}\text{Br} + ^{148}_{57}\text{La} + ^1_0\text{n} \tag{1a}$$
$$\rightarrow ^{94}_{36}\text{Kr} + ^{139}_{56}\text{Ba} + 3^1_0\text{n} \tag{1b}$$

Notice that the above reaction equations are written as balanced equations in both numbers of nucleons and charge. However, if you look in a table of precise mass values, you will find for the nuclear masses of the entries in the first reaction:

$$M(^{235}_{92}\text{U}) = 235.11240$$
$$M(^{87}_{35}\text{Br}) = 86.95722$$
$$M(^{148}_{57}\text{La}) = 147.98930$$

These values imply a mass loss of 0.16588 mass units in the reaction. Using the Einstein mass-energy equivalence, this calculates to 155 MeV of energy which, according to the energy conservation principle, must show up as kinetic energy distributed among the reaction fragments. This is a very large amount of energy when compared with that of ordinary nuclear processes such as alpha, beta or gamma decay (1–10 MeV), and especially when compared to chemical reactions (∼5 eV).

A second notable feature of fission reactions is that neutrons are released as debris. Shortly after the discovery of fission, careful measurements in several laboratories proved that the average number of neutrons released per fission is more than one. It was then apparent that under appropriate circumstances these neutrons could initiate fission of other $^{235}_{92}$U nuclei and that the physical basis for a nuclear chain reaction exists. The possibilities for practical nuclear power generation and for weapons were immediately recognized by experts all over the world, and a race began. The first controlled nuclear chain reaction was achieved in 1941 at the University of Chicago by a team under the direction of Enrico Fermi, and the first bomb was exploded in 1945.

Nuclide	ν	η_{therm}	η_{fast}
$^{233}_{92}$U	2.50	2.27	2.60
$^{235}_{92}$U	2.43	2.06	2.18
$^{239}_{94}$Pu	2.90	2.10	2.74

TABLE I. Number of neutrons liberated per neutron capture in fissile material. In the table, ν is the neutrons liberated per thermal neutron induced fission, η_{therm} is the neutrons liberated per thermal neutron absorbed, and η_{fast} is the neutrons liberated per fast neutron absorbed.

Table I lists the average numbers of neutrons released in various fissile materials. In this table, the differences between ν and η (defined therein) arises because neutrons are sometimes captured without producing fission.

For technical reasons of efficiency and control, most nuclear reacting systems operate so that the neutrons which produce the fissioning are "slow", *i.e.* have very low kinetic energy. On the other hand, the neutrons which are released in the fission process are "fast" neutrons with relatively high kinetic energy, on the average about 1.5 MeV. Thus they must be slowed down (or moderated) to a low energy. This can be done by elastic scattering of the neutrons from light atoms in a cool *moderator*. Each scattering reduces the energy of a neutron until its energy approaches the mean energy of the moderator atoms in
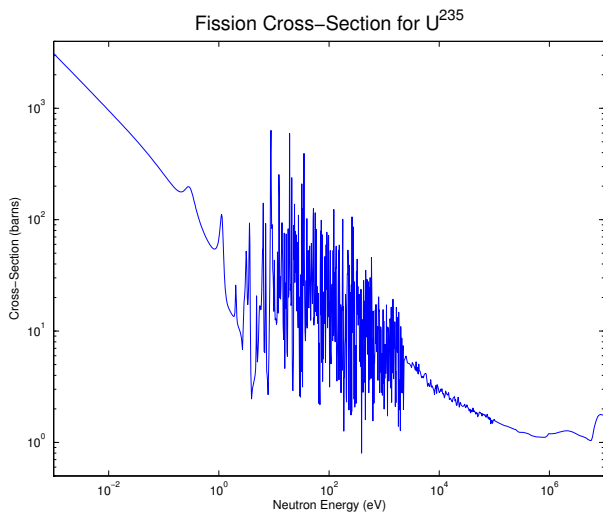
FIG. 1. Schematic fission cross-section for $^{235}_{92}$U. Data from atom.kaeri.re.kr/ton.

Nuclide	Fission (barns)	Capture (barns)	Capture/Fission ratio
$^{232}_{90}$Th	—	7.4	—
$^{233}_{92}$U	527	54.	0.102
$^{235}_{92}$U	577	106.	0.184
$^{238}_{92}$U	—	2.7	—
$^{239}_{94}$Pu	742	287.	0.387

TABLE II. Thermal neutron cross-sections for nuclear materials.

I.2.   Design Features of a Nuclear Reactor

In the preceding section, we have surveyed some of the physical concepts and parameters that are of significance in thinking about a nuclear chain reaction. Of course, this is far removed from answering the question, "how to make it work?". Many different reactor designs have evolved, each one aimed at achieving certain objectives. *Research reactors* produce radiation, radionuclides or other products useful in scientific and medical studies; *power reactors* produce energy for practical use; *production reactors* use excess neutrons to transmute the abundant non-fissionable isotope of uranium, $^{238}_{92}$U, into fissionable plutonium, $^{239}_{94}$Pu for weapons.

Components of a reactor that are common to all designs include:

Fuel Elements: Either natural uranium or uranium enriched in the isotope $^{235}_{92}$U, usually in the form of uranium oxide or alloyed with aluminum and sealed in aluminum tubes or plates.

Moderator: Frequently light or heavy water, but in some cases graphite or beryllium.

Thermal Heat Transfer System: Removes the heat generated by conversion of the kinetic energy of the fission fragments. The latter are entirely retained in the fuel elements.

Control Elements: Neutron absorbing elements such as cadmium are used to control the neutron flux density and hence the rate of the chain reaction and power output of the reactor.

Surrounding Radiation Shield: Intense neutron and gamma radiation, produced by the fission process and the radioactive decay of fission fragments, must be contained by shielding.

The simplest spatial configuration of these components would be many small fuel elements positioned in a spatial lattice and immersed in a liquid moderator which is circulated through an external heat exchanger to dissipate or utilize the heat generated by the process. To maintain the desired power level thermometers and/or radiation

accordance with the equipartition theorem of statistical physics. Carbon in the form of graphite was used as the moderator in Fermi's first reactor. Light water (H_2O) is now commonly used (as in the MIT reactor). Analysis shows that, on the average, one needs about 18 scattering events with hydrogen nuclei (protons) to reduce the neutron energy from 1.5 MeV to a typical thermal energy of 1/40 eV at which point further scattering events can raise as well as lower the neutron energy. The thermal equilibrium is characterized by the physical temperature of the moderator (about 50°C at MIT, but much higher in a power-producing reactor).

The efficiency of neutrons in producing fission depends upon the neutron energy and is conventionally described in terms of the *fission cross section*, or effective target area of the fissioning nucleus, expressed in *barns* (a picturesque name for 10^{-24} cm^2). The dependence of this upon neutron energy for the case of $^{235}_{92}$U is shown in Figure 1 which displays a nice distinction between commonly-designated neutron groups: slow or thermal (< 0.1 eV), resonance (0.1–1000 eV), and fast ($> 10,000$ eV). Note particularly the much higher fission cross section for thermal neutrons. Neutron physics is sometimes studied in regimes beyond the above classes, in particular as cold or ultra-cold ($\approx 10^{-7}$ eV). Ultra-cold neutrons (UCN) exhibit very interesting properties. For example, in a life-time measurement of UCN it was found that they cannot penetrate surfaces and can be contained in an experimental "bottle"!

An important quantity for reactor design purposes is the fission cross section at the thermal energy which is attained by most of the neutrons after moderation. For a moderator kept at temperature T (absolute Kelvin), the thermal energy is kT and at room temperature this is about 1/40 eV. The cross sections for fissionable nuclei are listed in Table II.

monitors would be connected to servo-mechanisms to adjust automatically the positions of cadmium control rods inserted into the lattice. Details of the particular features of the MITR-II will be provided to you at the time of your practicum. Useful references on nuclear engineering and reactors include [2–4].

I.3. Bragg Diffraction of Neutrons and the De Broglie Relation

See Bragg (1915) [5].

In the early years of the twentieth century, physicists were faced with the wave-particle dilemma in describing the properties of the electromagnetic field and how it interacts with matter. Young's interference experiments with visible light (1801), Hertz's experiments with radio waves (1887), and von Laue's discovery of x-ray diffraction (1912) showed wave interference and provided measures of wavelength for electromagnetic radiation from radio to x rays. On the other hand, Planck's theory of the black-body spectrum (1901), and Einstein's theory of the photoelectric effect (1905) showed that electromagnetic radiation is *absorbed* at a surface in discrete amounts of energy (quanta) and not as a continuous flow. Bohr's theory of the hydrogen atom (1913) showed that electromagnetic energy is *emitted* in discrete quanta. And, finally, Compton's interpretation of his own experiments on the incoherent scattering of x rays (1923) showed that x rays of wavelength λ interact with free electrons like particles with energy hc/λ and momentum h/λ. A composite picture was thus formed in which electromagnetic radiation is characterized by the seemingly contradictory concepts of wave frequency and wavelength, and particle momentum and energy.

Recognizing this interrelation for photons between wave and dynamical properties, De Broglie suggested in 1924 (in his PhD thesis) that similar properties should characterize all particles of matter. At that period, matter was considered to be made up of electrons and protons. This meant that electrons and protons (or any composite of them like an atom, a baseball, or the Earth) in motion should possess a wave character. De Broglie proposed a relation between the wavelength λ and momentum mv:

$$\lambda = \frac{h}{mv}, \tag{2}$$

where h is Planck's constant. This relation is the same as for photons, with, however, the recognition that photon momentum obeys $p = E/c$ (with the photon energy $E = h\nu$ and ν the electromagnetic wave frequency).

Although not taken too seriously at first — it is reported that Einstein himself was incredulous initially — De Broglie's suggestion was given full acceptance with the discovery of electron diffraction by G. P. Thompson and by Davison and Germer in 1927. They drew upon the fact that atoms in a crystal are positioned relative to each other in a very regular way, and that their

spacing is a few Angstroms ($1\text{Å} = 10^{-10}$ m) in scale. Their experiments on the reflection of electron beams from metal crystals demonstrated that wave interference effects were obtained with electrons of an energy such that their De Broglie wavelength is comparable to the separation of the crystal planes, a result completely analogous to that previously observed with x-ray photons (which certainly were endowed with a wavelength) and interpreted by Laue and Bragg. Since that time, further confirmation of the wave-particle duality has come for other types of particles (waves) such as alpha particles, atoms, neutrons and mesons. We shall see this duality in full display in Section I.3 of this experiment, where we shall again directly measure the velocity of a group of neutrons and at the same time observe the diffraction of these same neutrons by a crystal, thereby establishing their De Broglie wavelength.

II. THEORY

II.1. Thermal Spectrum Theory

The Maxwell-Boltzmann distribution law describes the distribution in speed (or kinetic energy or momentum) of atoms in a gas in a state of thermal equilibrium. Neutrons within the reactor can be expected to obey a similar distribution law, namely

$$n(v)dv = \frac{4N}{\sqrt{\pi}} \left(\frac{v^2}{v_0^3} \right) \exp\left(-\frac{v^2}{v_0^2} \right) dv, \tag{3}$$

where v is the neutron speed, v_0 is the most probable speed (*i.e.* the peak of the speed spectrum), N is volume density of all neutrons (*i.e.* neutrons/volume), $n(v)dv$ is the neutron density for those with speeds falling in the speed interval between v and $v + dv$. (See texts on gas kinetic theory, *e.g.* Reference [6, 7].)

This can be recast in terms of other kinetic parameters such as kinetic energy E for which we have

$$E = \frac{1}{2}mv^2 \qquad \text{and} \qquad dE = mvdv, \tag{4}$$

yielding

$$n(E)dE \propto \left(\frac{E}{E_0} \right)^{1/2} \exp\left(-\frac{E}{E_0} \right) dE, \tag{5}$$

with

$$E_0 = \frac{1}{2}mv_0^2 = kT, \tag{6}$$

where m is the neutron mass.

The corresponding flux density in the collimated beam, *i.e.* the number of neutrons per unit area per unit time with velocity between v and $v + dv$ passing a given point, is

$$\begin{aligned} j(v)dv &= vn(v)dv \\ &= J_0 v^3 \exp\left(-\frac{v^2}{v_0^2} \right) dv. \end{aligned} \tag{7}$$

As mentioned above, the neutron detector is a "thin" counter for which the efficiency e varies with neutron speed as $1/v$. Thus

$$e = A(1/v), \qquad (8)$$

with A being some constant. If we now call $j'(v)dv$ the number of *detected* neutrons per unit area of detector per unit time with velocity between v and $v + dv$, then

$$j'(v)dv = Bv^2 \exp\left(-\frac{v^2}{v_0^2}\right) dv, \qquad (9)$$

where B is a constant. Can you figure out the reason for using a "thin" counter rather than using one with higher efficiency of say 50%, aside from the fact that we don't need the higher efficiency because the measured intensity is adequately high?

In the experiment you will perform, the quantity actually measured by the apparatus in each event is not the velocity, but rather the time interval between a fiducial "start" signal from a photodetector and the detection of a neutron by a BF_3 detector. The accumulated data is then the number N_i of neutrons detected in the ith time channel, corresponding, after appropriate calibration and zero-time correction, to a flight time t_i. Since $L = vt$, we have

$$N_i = D\left(\frac{1}{t_i^4}\right) \exp\left(-\frac{L^2}{v_0^2 t_i^2}\right) \Delta t, \qquad (10)$$

where Δt is the finite and constant width of a the time channels, t_i is a flight time within the ith interval, and D is a constant.

Note that

$$\ln(t_i^4 N_i) = -\left(\frac{L}{v_0}\right)^2 \left(\frac{1}{t_i}\right)^2 + \text{constant}, \qquad (11)$$

or, equivalently, that

$$\ln\left(\frac{N_i}{v_i^4}\right) = Q - \frac{v_i^2}{v_0^2}, \qquad (12)$$

where Q is a constant. Thus a display of the quantity (N_i/v_i^4) against v_i^2 on semi-log scale should be a straight line with negative slope $(1/v_0^2)$. It will be convenient to display the data in this way to check the validity of the Maxwell-Boltzmann distribution and to evaluate v_0 and T.

II.2. Bragg Diffraction of Neutrons and the De Broglie Relation

We shall require some facts about crystals and the wave interference effects that may be observed with them. As mentioned above, a crystal represents a collection of many atoms bound together by inter-atomic forces to form a three-dimensional solid. (However, two-dimensional cases and liquid crystals are known to exist.)
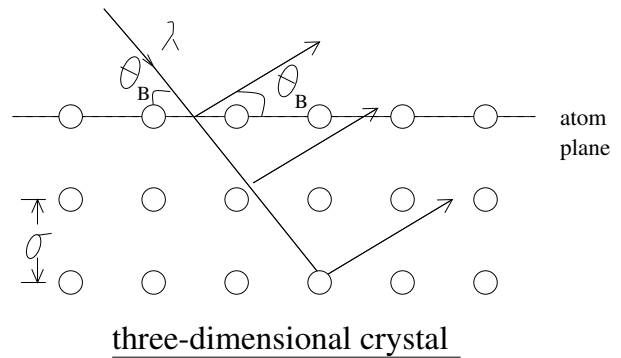

three-dimensional crystal

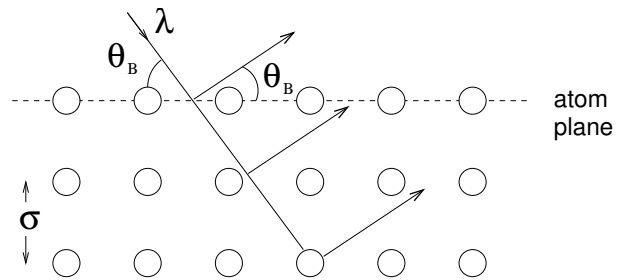FIG. 2. Schematic representation of a crystal with rows of atoms extending into the page.

FIG. 3. Schematic representation of a diffraction grating as a one-dimensional set of scattering centers.

In a perfect crystal, the atoms are positioned in a spatial array (or lattice) with precision, this being determined by the symmetry and balancing of inter-atomic forces on each atom. With this regularity of position, illustrated schematically in Figure 2, it is easy to envision the overall crystal as being made up of parallel sheets (or planes) of atoms which can serve to provide wave interference between the components of radiation scattered by individual atoms. Almost any textbook on modern physics (*e.g.*, reference [8, 9]) will have an elementary derivation of the conditions necessary for constructive interference of radiation scattered from atoms in a crystal plane. These conditions are expressed by Bragg's law,

$$n\lambda = 2d\sin\theta_B, \qquad (13)$$

where $n = \{1, 2, 3, \ldots\}$ is the order of diffraction, λ is the wavelength, d is the interplanar spacing, and θ_B, called the Bragg angle, is the grazing angle of incidence and reflection. It is deceptively similar in appearance to the law describing constructive interference from a one-dimensional set of scattering centers (*e.g.* a grating), and it is worth pointing out the difference.

In the one-dimensional case, illustrated in Figure 3, the approach angle θ_1 may have any value, and the exiting angle θ_2 for constructive interference is then defined by the interference equation with θ_2 not necessarily equal to θ_1. For reasons not so obvious, this generality is not present in three-dimensional diffraction where $\theta_1 = \theta_2 = \theta_B$. In fact, diffraction from a crystal al-
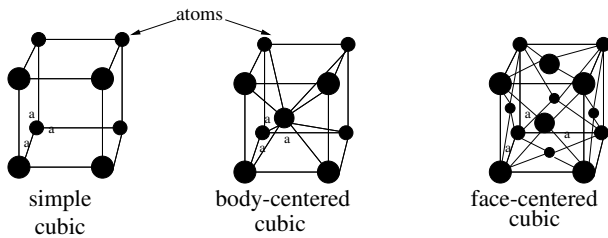
FIG. 4. The three forms of cubic crystals.

FIG. 5. Diagrams showing how Miller indices are used to define crystal planes.

ways occurs in symmetrical fashion from atom planes with both incident and emergent angles being equal to θ_B. (This subtle distinction is discussed in [10] and in various texts on crystallography, *e.g. X-Ray Crystallography*, M. Wolfson, Cambridge 1970.) A given set of atom planes of spacing d will reflect radiation of wavelength λ with intensity concentrated in a narrow range of angles (typically within 10^{-5} radians) with a maximum at the Bragg angle θ_B defined above. This is not true for the one-dimensional grating where, for any incident angle θ_1, diffraction maxima occur at angles θ_2 given by the formula in the figure, provided $d > \lambda$.

II.3. Crystallography

A crystal may be considered as being made up of an infinite number of different atom plane layers, each set with a different interplanar spacing and different orientation. Bragg diffraction can occur from any of these sets as long as the Bragg law is satisfied. What we need at this point is a shorthand method of classifying these different sets of planes, which we now develop. Since nature causes atoms to pack together in different ways (but always in a given way for a given species of atoms or molecules; a change of external conditions such as the temperature, pressure, or magnetic field application can invoke a change of structure, a *phase transition*), it is apparent that many different forms of crystal structure may be encountered. These are classified according to symmetry characteristics: cubic, hexagonal, orthorhombic, *etc.* Common to all forms is the concept of the *unit cell* which represents the smallest collection of atoms (or molecules) which, when repeated along the three axes, make up the whole crystal. Thus cubic crystals have cubic unit cells and the size of the unit cell a_0 is set by one dimension. However, cubic cells may contain any one of three different atom configurations as shown in Figure 4.

For the general case, the unit cell can be defined by three vectors a, b, and c directed parallel to the unit cell edges and of magnitude equal to the size in that direction. Furthermore, we can identify the orientation of any plane of atoms in the crystal by the intersections of this plane with the three axes of the unit cell. It is a great convenience to do this in terms of the *Miller indices* h, k, and l (small integers) with a/h, b/k, c/l being the intersection points of the plane with the respective axes,
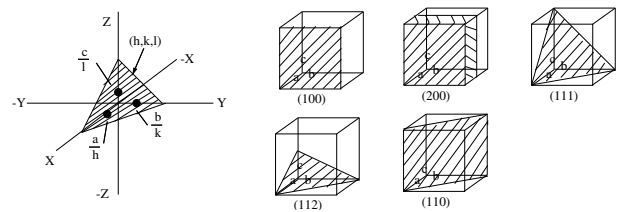
as illustrated in Figure 5.

We label a particular set of atomic planes as being (hkl) planes according to these Miller indices. A little geometry will show, for the case of a cubic crystal, that the interplanar spacing d_{hkl} will be given simply by

$$d_{hkl} = \frac{a_0}{(h^2 + k^2 + l^2)^{1/2}}. \quad (14)$$

In our experiment, we shall be using a metal crystal of pure copper which has a face centered cubic structure (four unique atoms per unit cell) with unit cell size $a_0 = 3.6147$ Å. Note that this value of a_0 may be calculated from the measured density $\rho = 8.939$ g·cm^{-3}, Avogadro's number 6.0221×10^{23} atoms per mole, the molecular weight 63.55 g/mole, and the number of atoms per unit cell. Check that this is so. Also calculate interplanar spacing values for planes (200), (220), and (111), which you will be using in the experiment. You should identify in the above figure of cubic unit cells just which atoms are unique to the unit cell. There are four for face centered cubic. (How many are there for the other cells?) Incidentally, some common elements like Fe, Cr, Na, and Mo crystallize as body centered cubic (BCC), while Cu, Al, Au, and Pb crystallize as face centered cubic (FCC). No element is known to exist in simple cubic form.

Before leaving our crystallographic considerations, we should investigate whether there are restrictions on the appearance of Bragg diffraction from the many (hkl) sets of planes. To illustrate this for our FCC case, a view of the unit cell normal to a face shows atoms and atom planes as shown in Figure 6. There are sheets of atoms separated by the fundamental distance $d(002) = a_0/2$, with common atomic density in all sheets. If we were to attempt to observe (001) diffraction as prescribed by Bragg's law, we would find reflected rays (A) and (C) to be in phase, as would (B) and (D), but the two groups would be *out of phase* with respect to each other, and hence overall destructive interference would occur. Thus zero intensity in (001) diffraction is expected, but finite intensity in (002) diffraction. Without going into detail, the general rule for an FCC structure is that *the Miller indices must be either all even integers or all odd integers in order for constructive interference to occur.* Thus there will be no (100), (110), or (221) diffraction occurring, but there can be (020), (111), (022), or (311) for FCC. Other crystal structures would have different selection rules.
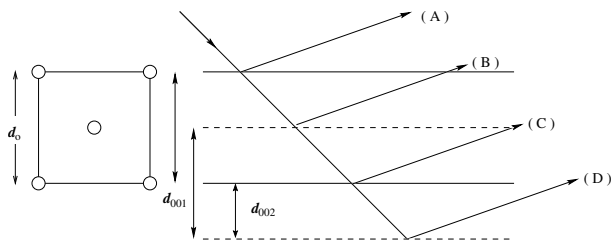
FIG. 6. Illustration of Bragg reflection from a FCC crystal in which destructive interference between reflections from adjacent (001) planes occurs.

Miller indices can be taken negative as well as positive, and a negative index is written as a bar over the index. Thus $(11\bar{1})$ would designate an allowed set of planes in the FCC structure Bragg diffraction.

III.   APPARATUS

III.1.   Time-of-Flight Spectrometer

In all of the present experimentation we shall use a pulsed, collimated beam of neutrons emerging from the reactor in a setup shown schematically in Figure 7. The distribution in energy of the neutrons in the beam reflects the equilibrium spectrum of the moderated neutrons in the reactor. In accordance with the principles of statistical physics, we anticipate that this spectrum is the Maxwell-Boltzmann spectrum characterized by a temperature that is the same as the physical temperature of the moderating agent in the reactor (normal water in the case of our reactor; some new reactor designs are employing molten salt instead), providing complete moderation of the neutrons has occurred. Thus we can think of the neutrons in the reactor as constituting a neutron gas in thermal equilibrium with the moderator, with a certain density and temperature. We will examine the velocity spectrum of the neutrons by letting some escape as a collimated beam through a small opening in the reactor shield.

We will measure the velocity spectrum by timing the flight of individual neutrons over a laboratory distance of about 1.25 meters. We do this by "chopping" the beam as it emerges from the reactor to produce periodic short bursts of neutron intensity. After traveling the flight distance ,the neutrons are detected with a small neutron counting tube, and the occurrence times of the individual counting pulses relative to the starting time of the burst are recorded with a multichannel scaler (MCS).

III.2.   The Neutron Chopper

The chopper is a slotted disk of neutron-absorbing cadmium which rotates about an axis above and parallel to
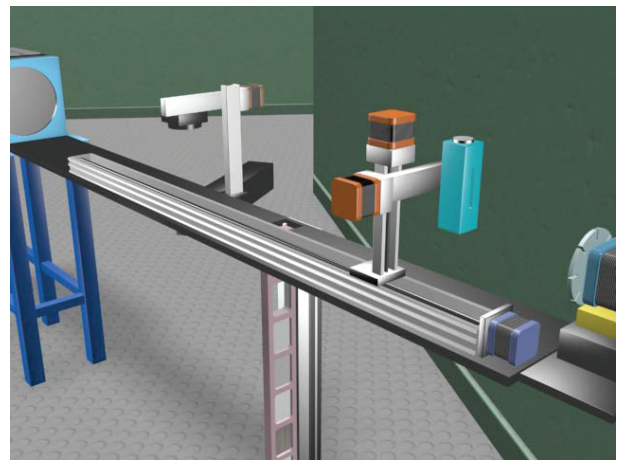

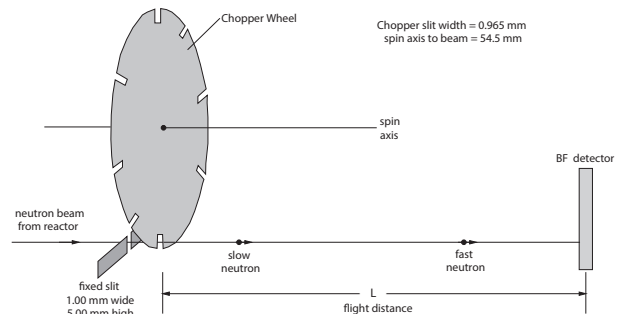FIG. 7. Experimental setup for time-of-flight spectroscopy at the MIT Nuclear Reactor. [11]

FIG. 8. Schematic diagram of the time of flight spectrometer showing the beam chopper and the BF₃ detector.

the neutron beam line, as illustrated in Figure 8. Cadmium is very absorptive to neutrons of energy less than about 0.40 eV (speed of 8760 m/sec), and serves as a good shutter for thermal neutrons. The cadmium disk of thickness 1 mm is sandwiched between two aluminum disks for mechanical stability. Around the periphery of the disk assembly, eight radial slots have been cut. The width of each slot is 0.95 mm. Immediately upstream of the chopper disk is a fixed slit opening made of neutron absorbing material (boron containing plastic) with width 1.00 mm and height 5 mm. This serves to define the beam size entering the chopper assembly. The axis of rotation is located 54.5 mm above the geometrical center of the defined neutron beam.

A small speed-controlled synchronous motor rotates the disk. Every time a radial slit passes the fixed slit, a burst of neutrons is admitted to the flight line. Since the slit widths are nearly equal, the time structure of intensity in this burst (which may contain several hundred neutrons) is triangular, with a full width at half maximum (FWHM) determined by the slit width and rotational speed. You should convince yourself of this feature. Also, consider what it would be for the case of unequal slits. The rotational speed of the synchronous

driving motor is fixed by the power line frequency and is seen as the neutron burst repetition rate in hertz. This frequency will be 480 Hz throughout the experiment.

It is necessary to establish a reference time for the origin of each of the neutron bursts. This is done by the periodic interruption of a light beam passing parallel to the neutron beam line between a tiny photodiode and photodetector which is positioned about 90° around the disk from the neutron beam. The geometry is arranged so that a light signal occurs a short time before each neutron burst. The light signal sets the time origin of the MCS used to measure the neutron flight time. Thus the actual neutron burst origin time is slightly later than the MCS origin time by a certain fixed delay which must be determined as a part of the experiment.

III.3.   The Neutron Detector

Small gas-proportional counters are used as neutron detectors. For the Maxwell-Boltzmann part of the experiment, the counter of choice contains BF_3 gas in a sealed aluminum tube of diameter 0.5 inch and length 3 inches. The neutron beam is located near the bottom (vertically) center (horizontally) of the BF_3 detector's range of motion. High voltage is applied between the metal tube and a fine center wire. The resulting electric field collects the charges produced by gas ionization caused by the energetic nuclei from the reaction $^1_0 n + ^{10}_5 B \rightarrow ^7_3 Li + ^4_2 He$. The $^{10}_5 B$ isotope forming 18.8% of natural boron captures neutrons with a large cross section that varies as $1/v$, where v is the neutron speed. Many nuclei, such as $^1_1 H$, $^6_3 Li$, $^3_2 He$, and $^{197}_{79} Au$ exhibit this "$1/v$ law" capture of slow neutrons (See the plot of the $^{235}_{92} U$ fission cross section in Figure 1.)

The counter contains BF_3 gas at a pressure of 550 mmHg; a typical neutron passing along a diameter will be detected with an efficiency of about 1%. (Note: this was true of older BF_3 detectors. However, the manufacturor of the present detector, LND, Inc, has yet to confirm the efficiency for this detector, but it could be as high as 20%). It is purposely selected to be thin (low efficiency) so that a simple analytical correction can be applied in the analysis of the spectral data. Electrical pulses from the counter are amplified in a preamplifier and in a main-line amplifier, selected by a single channel window analyzer, and counted by a scaler. Thereafter they are sent to an oscilloscope for observation, and to an MCS for arrival time sorting. The output pulses from the amplifier are about 5 μs in duration.

III.4.   Bragg Scattering Crystal

The copper crystal used in the Bragg scattering experiment has been grown and cut in the form of a small disk of diameter about 15 mm and thickness about 2.3 mm. Copper metal usually exists in polycrystalline form, *i.e.*,

it is made up of many microscopic crystallites (perhaps about 1 μm in size) oriented at random. Our single crystal has been prepared in a special way (called the Bridgman method): the metal was melted in a crucible of special shape, and the temperature was very slowly reduced through the freezing temperature with a controlled temperature gradient. This permits a single crystal to grow to a size limited only by the crucible dimensions (if the conditions are right!). Our crystal disk has been cut from such a grain after establishment of the grain orientation by diffraction techniques (neutrons, of course!). The flat faces of the disk have been cut and surface polished to high precision—they are parallel to the (110) crystallographic planes to within 1 arc minute. Looking down on the crystal disk, we see the unit cell as illustrated in Figure 10.

In testing the De Broglie relation, we shall use diffraction from the (002) planes which are accurately perpendicular to the (110) faces. Thus we shall be using the disk in transmission orientation, *i.e.*, the neutrons will pass symmetrically through the disk. Copper is relatively transparent to neutron radiation with an absorption cross section of 3.69 barns for thermal radiation of speed 2200 m/sec. You should calculate the intensity loss this implies.

The crystal disk has been attached to a support plate with the (002) planes vertical.

IV.   MEASUREMENTS

The three primary measurements to perform are: the Maxwell-Boltzmann distribution measurement, Bragg scattering of thermalized neutrons and the De Broglie relation, and finally neutron absorption cross sections.

IV.1.   Maxwell-Boltzmann Experimental Procedure

1. Start up and examine the hardware.

   (a) Examine the apparatus and, with the aid of an instructor, identify the components and their functions. Note the bias voltages of the BF_3 detector (should be around +1000 VDC) and the He-3 detector (should be around +1600 VDC). Also note the settings of all amplifiers. You should not need to adjust these settings, but you will want to note them so that you can tell if they have been changed between your experimental sessions. If you do change them for your measurement, be sure to return them to the previous settings before you leave your session.

   (b) Log in to the control computer using the instructions in the *Neutron Spectrometer Operation Manual.*

(c) If not already open, have your reactor escort open the shutter to admit the neutron beam to the apparatus. A yellow "beam-condition" warning light will be activated. The neutron beam is fully exposed until it is finally absorbed in a beam stop at the end of the flight path. **The beam is of high intensity and exposure of any part of the body to it must be avoided**. In addition to the thermal neutrons used in this experiment, there are also gamma-rays and unmoderated fast neutrons which are damaging to tissue.

2. Find the center line of the beam.

   (a) Using the LABVIEW program described in the *Neutron Spectrometer Operation Manual*, raise the chopper wheel and move the BF$_3$ detector as close as possible to the beam port.

   (b) Scan the detector position across the beam until the count rate is maximized, indicating the position of the beam's center line. This can be done using the Beam Scan sub-program. Carefully note this position for later use.

   (c) Examine the neutron detection pulses from the amplifier on the oscilloscope screen, noting their time width.

3. While you have the counter at the "near" position close to the chopper, you can measure the intensity of the beam. Using the formulae given in Appendix C, along with the known geometrical factors, you use this intensity to calculate an approximate value for the neutron flux and the neutron density inside the reactor.

   (a) With the chopper wheel still raised and the BF$_3$ detector on the center line of the beam, measure the intensity of the beam using the Counter sub-program. (The BF$_3$ is indicated as the "Low-Efficiency Detector".) Integrate counts until your uncertainty on the mean count rate is around 1%.

   (b) Lower the chopper wheel and stop its rotation so that the rate of background gamma radiation and neutrons which are not stopped by the cadmium in the wheel can be measured. The wheel may take several minutes to stop spinning. In the unlikely case that the wheel stops with the slits aligned, then raise and lower the wheel a few times until the alignment is broken. Again, use Counter sub-program to establish the count rate in this position. The difference between these average count rates, divided by the detector efficiency gives the thermal neutron intensity expressed in neutrons per second.

4. Measure the time-of-flight spectrum in the "near" position.

   (a) Lower the chopper wheel and activate the chopper motor. Wait until it settles to the rotational speed corresponding to a neutron burst frequency of 480 Hz.

   (b) The Multi-Channel Scaler (MCS) that you will be using is part of the LABVIEW program interface. The presets should be set as follows:

   - Dwell time: 2 μs
   - Pass Length: 1000
   - Pass Count: 432,000

   The dwell time (seconds per channel) multiplied by the pass length (channels) must be less than the time interval between consecutive neutron bursts. Your data is saved in the file created during the start-up of the LABVIEW program. Before long runs be sure to verify where the data is saved. The data can also be copied directly from the data tab in the MCS sub-program.

   (c) Set the MCS into operation and note the build-up of neutron counts in early time channels of the MCS time display. Since the flight distance is so small (only about 5 cm), neutrons of different speed do not have a chance to spread apart before detection. Collect data over a recorded time interval and stop the collection.

5. Move the BF$_3$ counter to the furthest position from the beam port along the flight channel. Again, note the build-up of neutron counts on the MCS display. Neutrons are now found in later time channels distributed over a time spectrum. Collect data for a recorded time interval. This will take about 40 minutes to get statistically meaningful numbers because the neutron counts are now spread over many channels. (The electronic cut-off of high channels is purposely introduced to eliminate overlap from one burst to another.)

6. Once you have completed your data runs, close the spectrometer program by pressing the QUIT button on the main screen. Locate your saved data file and copy it to a convenient location for future analysis.

IV.2. Bragg Scattering Experimental Procedure

We shall use the same neutron beam as described in Section III.1. As we have seen, it is a full spectrum beam with all neutron speeds (or as De Broglie asserted, all wavelengths). However, before detecting it on its normal straight flight line, we shall interrupt it with a diffracting crystal of copper. After repositioning the detector, we can detect the Bragg diffracted beam in the direction
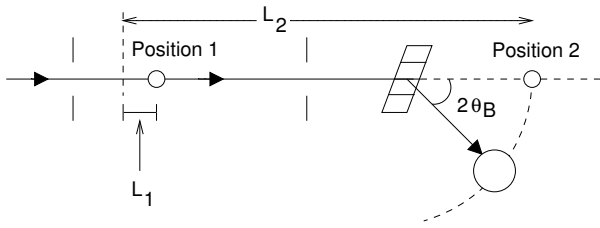
FIG. 9. Schematic diagram of the neutron beam diffracted from the copper crystal. The distance from the chopper to the crystal is 33.63±0.06 inches. The distance from the crystal to the detector is 20.00 ± 0.06 inches.
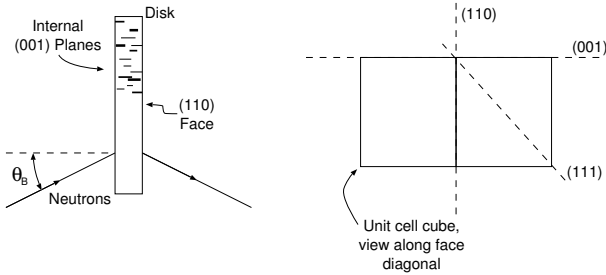

FIG. 10. Illustration of the orientation of the crystal planes in relation to the geometrical shape of the crystal.

that makes an angle of $2\theta_B$ with the incident beam, as shown in Figure 9.

The copper crystal will be positioned along the neutron flight line, somewhat in front of the position where you placed the detector for the Section IV.1 spectrum measurement. Notice that there is a fixed slit opening (of width 3.0 mm) just before (upstream from) the crystal position, and this serves to further define the direction of neutron ray trajectories — along with the fixed slit in front of the chopper disk shown in Figure 8 — which can hit the crystal.

If a particular set of crystal planes (hkl) is oriented at an angle θ_B from the incident beam direction, neutrons with wavelengths in a narrow band will satisfy Bragg's law and hence be diffracted at angles in a narrow range around $2\theta_B$ from the incident beam direction. We can detect this diffracted beam by placing our detecting counter at the appropriate angular position. In our experiment, we shall select various orientation positions of the crystal (thereby selecting θ_B) and simultaneously measure the flight time of the diffracted neutrons which arrive at the detector. This provides both the wavelength λ (from the Bragg law) and the velocity v of the diffracted neutrons. By changing the crystal orientation (and the detector position), we can scan over a range of λ and v and test the De Broglie relation in a very direct way.

Instead of using the low efficiency, thin BF$_3$ counter that was used in the Section III.1 spectrum measurement, it will be helpful to use a high efficiency (about 90%) counter with $^3_2$He gas. This is similar in operation to the BF$_3$ counter, but it contains isotopic $^3_2$He gas at

high pressure, about 40 atmospheres. $^3_2$He is the very rare and expensive isotope of elemental helium. As with boron, $^3_2$He also exhibits a $1/v$ absorption cross section for neutrons. The same counting circuit will be used, but different counter voltage and amplifier gain settings will be needed. These conditions will be posted locally.

1. Set the crystal orientation so that the (002) planes have $\theta_B = 20°$. Leave the chopper motor off and put the wheel in the up position.

2. If not already open, have your reactor escort open the shutter so that a steady neutron beam falls on the crystal. A yellow "beam-condition" warning light will be activated. The neutron beam is fully exposed until it is finally absorbed in a beam stop at the end of the flight path. **The beam is of high intensity and exposure of any part of the body to it must be avoided**. In addition to the thermal neutrons used in this experiment, there are also gamma-rays and unmoderated fast neutrons which are damaging to tissue.

3. Without disturbing the crystal orientation, move the counter in angle position around $2\theta = 40°$ using the Crystal Angle Scan sub-program. With Bragg diffraction occurring at the crystal, we expect a localized intensity peak at about 40° scattering angle. Measure the intensity with short time counting in the electronic scaler at different positions of the detector using steps of 0.25°. Examine this plot this immediately, and determine the center position.

4. Set the chopper wheel in motion and wait until it stabilizes at the 480 Hz burst rate, as before.

5. *Time saving hint*: Read Appendix B and do transmission cross-section measurements as part of the next step.

6. Collect data in the MCS giving the flight time spectrum of the neutrons which are diffracted from the (002) planes in the crystal. There should now be a sharp peak at the flight times of the selected monochromatic neutrons. You may also see a lower intensity peak characteristic of $\lambda/2$ in second order diffraction from the same planes. Collect MCS data until you have good signal above background. This will take significantly longer than in the Maxwell-Boltzmann measurements you made earlier. If you see second order peaks in the MCS display, collect enough data to determine their flight time as well as for the first order.

7. Repeat for other selected θ_B values: 30°, 25°, 20°, and 15°. In setting other θ_B positions, it is worthwhile to redetermine the counter position as in Step 3 above. An off-center detector will produce an error in the measured speed relative to that expected from the Bragg angle of the crystal. You

expect the scattering angle to be close to $2\theta_B$ in each case. Remember that the θ_B value read on the more accurate goniometer is the primary angle quantity and the counter position is not of use in the later analysis. You want only to have the counter in the central part of the diffracted beam.

8. Once you have determined the central position for each angle and measured the spectrum at that angle, you may want to take a second spectrum through the boron absorber (pyrex beaker-bottom) for each angle. You will use these data for checking the $1/v$ dependence of the cross section for boron in Section IV.3.

9. You cannot safely access the containment area to measure the flight path distance from the chopper wheel to the counter center; it is different than in Section III.1. Use the following values:

   • From the chopper to the crystal is 33.63 ± 0.06 inches.

   • The distance from the crystal to the detector is 20.00 ± 0.06 inches.

IV.3.   Transmission of Slow Neutrons Through Materials

There are a number of other experiments that you can perform with the simple one-axis spectrometer. (More elaborate, sophisticated spectrometers sometimes involve three axes of scattering in research studies.) You may have time in the schedule to do at least part of the following, or you may discover additional measurements to perform. The monochromatic diffracted beams from the copper crystal are of low intensity (unlike the hot, direct white beam), and are safe to experiment with.

Most materials are relatively transparent to slow neutrons. This arises because neutrons carry no Coulombic charge (experiments have shown this to be less than 10^{-21} electron charges!), and thus they don't interact with the charge distribution in atoms by means of the long-range Coulombic interaction. They do interact with the nuclei of atoms through the short-range nuclear force interaction, and this is conveniently quantified by a nuclear scattering cross section (σ_S) and a nuclear absorption cross section (σ_A). Scattering cross sections do not vary very much from nucleus to nucleus and have values of a few barns (10^{-24} cm^2). On the other hand, capture or absorption cross sections vary widely depending upon the distribution of nuclear energy levels and thus nuclear resonance effects may be encountered. In illustration of this, we may note that the absorption cross section of carbon for thermal neutrons is only about 0.0034 barns, whereas for some exotic rare-earth nuclei this becomes as large as several million barns. Absorption cross sections invariably are sensitive to neutron energy — the
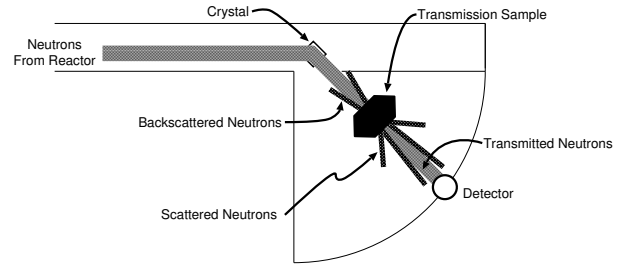

FIG. 11. Plan view of the experimental setup for measuring the attenuation of monoenergetic neutrons in a sample.

$1/v$ law mentioned earlier is a mild example of this — and resonance behavior is not uncommon.

You can study some of these cross sections by using the monochromatic Bragg diffracted beam from the copper crystal and establishing the transmission T of a piece of material for this beam, as illustrated in Figure 11. By definition,

$$T = \frac{I \text{ (intensity passed through the sample)}}{I_0 \text{ (intensity incident on the sample)}}. \quad (15)$$

This can be shown to be

$$T = \frac{I}{I_0} = \exp\left[-\sum_i M_i \sigma_{iT}\right] \quad (16)$$

with the index i symbolizing different nuclear species in a composite sample, σ_{iT} the transmission cross section (the sum of both σ_S and σ_A) per nucleus of the ith species, and

$M =$ areal density of nuclei

$\quad =$ number of nuclei/cm^2 sample

$\quad =$ volume density of nuclei · sample thickness.

Plate samples of Fe, Al, Cd, and boron-containing Pyrex glass are available for transmission cross section study. For Fe and Al, the transmission is dominated by the scattering process — hence, it is relatively insensitive to neutron energy — whereas for Cd and B, absorption dominates with significant dependence upon neutron energy. You will generally want to spend longer periods collecting intensity data through the sample than without. See Appendix B for notes on transmission measurements. Study all samples at fixed wavelength corresponding to $\theta_B = 20°$ as well as the boron sample at several wavelengths (energies).

The intensities to be used in obtaining T are best established from the MCS flight time spectral print-out. By summing the intensity in all channels over the monochromatic peak (corrected for background, of course), you obtain the integrated intensity in the Bragg reflection. Normalize these to a common data-collection time interval in getting T. With the Pyrex plate, the strong absorption cross section of B dominates, and you can establish

the $1/v$ law for this by measuring the transmission over a range of neutron velocities. Compare the established values for the cross sections with what you determine from experiment. Perhaps you have something else to place in the neutron beam whose transparency to neutrons you would like to assess. For instance, a thin plate of plastic (containing lots of hydrogen) will attenuate the neutron beam about as much as the thick iron plate!

V.   ANALYSIS

The procedures detailed in this section are readily accomplished using MATLAB on Athena or some other mathematical package of your choice.

V.1.   Maxwell-Boltzmann Data Analysis

1. Plot your data for the small distance case, neutron counts *vs.* channel number, and determine the center position and uncertainty. Is the shape what you expect, and does the FWHM agree with what you calculate? Remember that the neutrons have had little chance to spread out. On the other hand, the finite flight time over your small distance has shifted this peak by a small amount relative to the neutron burst origin time. You can correct for this shift by making use of the observed travel time of the peak in the MCS display for neutrons going from L_1 (the short flight distance) to L_2 (the long flight distance). Thus the correction is

$$\frac{L_1}{(L_2 - L_1)}(C_{2p} - C_{1p}), \qquad (17)$$

and the neutron time origin channel C_0 becomes

$$C_0 = C_{1p} - \frac{L_1}{(L_2 - L_1)}(C_{2p} - C_{1p}). \qquad (18)$$

Here, C_{1p} is the MCS channel of the center of the approximately triangular distribution obtained when the detector is at the near position; C_{2p} is the MCS channel position for the peak of the distribution recorded when the detector is at the far position which is at a distance L_2 and correspondingly for C_{1p}. It is interesting to note that the speed of the neutrons in the peak in the MCS time distribution

$$N_i = C \left(\frac{1}{t_i^4}\right) \exp\left(-\frac{L^2}{v_0^2 t_i^2}\right) \Delta t, \qquad (19)$$

becomes $\sqrt{2}v_0$, as you can establish by setting its time derivative to zero, thereby obtaining t_{peak}, and looking at this dependence on L. This can be compared to the peak in the velocity distribution which is v_0.

Note that the channel spread about the peak centered at C_0 (in the data taken at the small distance position) is a direct representation of the time resolution of the system. All later measurements are smeared by this limiting time resolution.

2. Plot a spectrum of your data as taken at the back counter position. Identify on your graph the neutron origin channel position C_0. All flight times are now established relative to this.

Create a plot of all the data points and an interpolated line. We expect that the spectrum will approach equal asymptotic levels at the two extremes of the spectrum, and that this is a background level by which all observed spectral intensity values should be corrected. Are the deviations of individual points from your smooth curve meaningful on statistical grounds? Remember that the collection of N statistically distributed events in a measurement means that there is 68% probability that the value N will fall within $\sqrt{N}$ of the true value as established by many repetitive measurements.

Since the expected Maxwell-Boltzmann spectrum approaches zero asymptotically at both extremes of the spectrum (because of the t^{-4} dependence at the high channel (low energy) end and the exponential dependence at the low channel end), the residual or base level that is observed represents a background intensity level arising from leakage neutron events not associated with opening or closing the chopper. Thus all observed intensities should be corrected by subtracting this background level. In assessing this background level for your data, you should note that $t \to 0$ for channels just above C_0 so the intensity level for channels just above C_0 should represent the base level. On the other hand, at the other extreme, near the electronic cut-off level of about channel 1000 (or whatever the number of channels has been set to in the MCS software), the Maxwell-Boltzmann spectrum has not completely collapsed to zero and the observed intensity may be somewhat higher that it would be for even lower channels. We can correct for this residual Maxwell-Boltzmann intensity in high channels by noting that its value, relative to the peak intensity depends upon v_0. **Previous experimentation has determined v_0, and calculation has shown that the ratio of this residual intensity in channels above 950 to that at the peak is 0.013.** Using this ratio value, determine the background base value which is most consistent with the observed intensity pattern at both ends of the spectrum. Pay no attention to intensity values corresponding to negative channel numbers (below C_0) since they are associated with transparency of the Cd in the chopper and with other leakage neutrons.

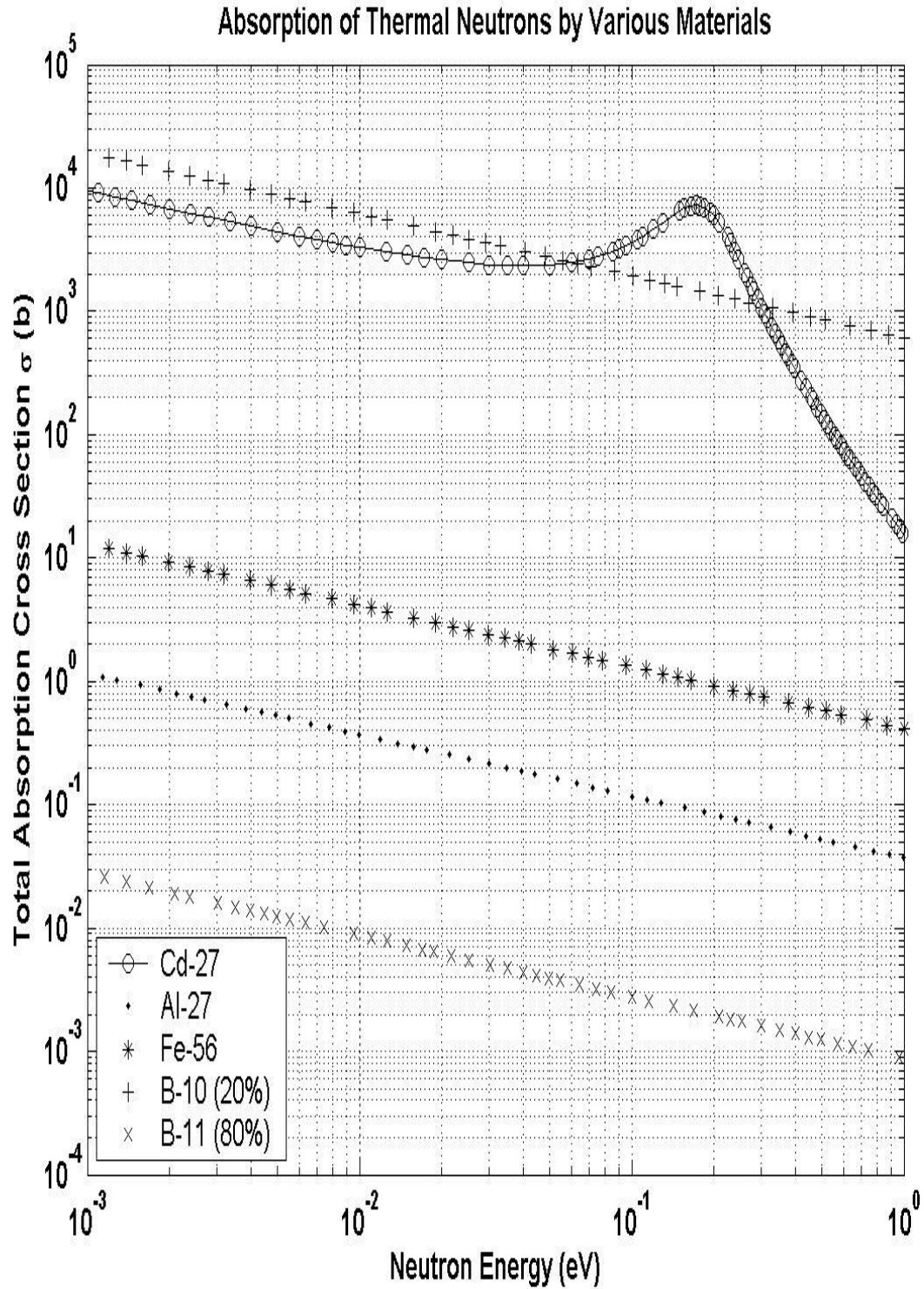3. Create data vectors of $N_{\text{observed}} - N_{\text{base level}}$ and

FIG. 12. Total absorption cross-sections for neutrons as a function of energy for B, Cd, Fe, and Al. Data from atom.kaeri. re.kr/ton. The percentages next to the Boron isotopes indicate their relative natural abundances.

corresponding $C_{\text{observed channel}} - C_0$. Follow with calculated values of the speed v using your measured flight distance and the individual channel time. Carry a number of significant figures that is consistent with the measurement precision.

Finally, tabulate values of $N_{\text{corrected}}/v^4$ and v^2. Make a semi-log plot covering about 3 log cycles of these quantities. According to our Maxwell-Boltzmann theory, these points should fall on a straight line whose slope is $1/v_0^2$. Graphical trick: to make full use of 3-cycle log paper, adjust your intensity data by an arbitrary multiplicative factor, as this will not affect the slope.

4. You will probably find that the high-velocity data points (> 5000 m/sec) in this semi-log display fall above a straight line fitted to the low-velocity data. Two effects contribute to such discrepancies:

   - The finite duration of the pulses of neutrons that emerge from the chopper causes a smearing of the observed velocity distribution so that it differs significantly from the true flight time distribution. (See if you can estimate the effect of this on your data.)

   - High energy neutrons generated in the fission process and encountering the relatively cold moderator are continually diffusing in "velocity space" toward lower velocity with the diffusion driven by an excess at high velocities over the equilibrium Maxwell-Boltzmann distribution.

Deviations from linearity of the plot may also occur at low velocities (< 1000 m/sec) for various reasons such as the high absorption cross sections of reactor materials for slow neutrons. It must be recognized, also, that the background intensity makes up a larger portion of the observed counting rates at the low and high-velocity ends of the data.

In any event, when fitting a straight line to the data, remember both effects and pay special attention to the main center region of the range. Since your physical judgment must establish the range of linearity, it is hardly worthwhile to use a least-squares fitting of the points to a straight line. Use your best judgment in this and estimate the uncertainty in the slope of the line. Do not hesitate to calculate values and plot additional points beyond your initial sampling of your smoothed spectral curve in assessing the best line fit. If you find gaps in your selected point distribution, analyze ad-

ditional intermediate ones which will help in recognizing the linear range.

5. Evaluate the slope of your best straight line and calculate v_0, $E_0 = 1/2mv_0^2$, and T from $kT = \frac{1}{2}mv_0^2$, and justify this relation. Recall in gases $E_{\text{kinetic}} = \frac{3}{2}m\bar{v}^2$. Does your neutron temperature T agree with that of the moderator? Does the peak position in the observed spectrum agree with that expected from your fitted parameters? From the uncertainty in the slope of the line, what are the uncertainties in these quantities?

6. Calculate the neutron flux and neutron density in the reactor from your data and the analysis in Appendix C. If we think of these neutrons as being confined in a walled container, what pressure would they exert on the walls?

V.2.   Bragg Scattering Analysis

Graph the time spectrum data obtained at the various θ_B selections. Only the peaks plus their nearby background are of interest here, including any small $\lambda/2$ peaks. Notice that the channel widths of these are essentially the same as your resolution width determined in Section III.1. Establish the centers of these peaks (use the steep sides of the peak in this), and correct for the neutron time origin C_0 determined above.

Calculate the wavelength and corresponding neutron speed (with significant figures consistent with the measurement precision) for the various monochromatic beam observations. Tabulate your data and graph v vs. $1/\lambda$ with scales including the origin. According to the De Broglie relation, your data points should fall on a straight line with slope h/m which passes through the origin. On your graph, draw the expected line using accepted values for h and m. This is an ideal case for applying a least-squares treatment of the line fitting. Anchor the fitted line at $v = 0 = 1/\lambda$ since the De Broglie law requires this.

Analyze the possible contributing errors that enter into your observations and establish the uncertainty in the slope of your linear fit. Is this consistent with the difference between your result and that expected from established constants? Typical runs show agreement to 1% or so.

Analyze the 2θ scans that you made in establishing the centered detector position in the Bragg reflection. Considering the ray geometry falling on the crystal and the angular width of the detector opening, this can tell you something about the perfection of the copper crystal.

[1] C. Shull and B. Brockhouse, "Nobel prize lecture," Nobel Prize Lecture (1994).

[2] A. Foster and R. Wright, *Basic Nuclear Engineering* (Allyn and Bacon, Boston, MA, 1977) tK9145.F754 Sci-
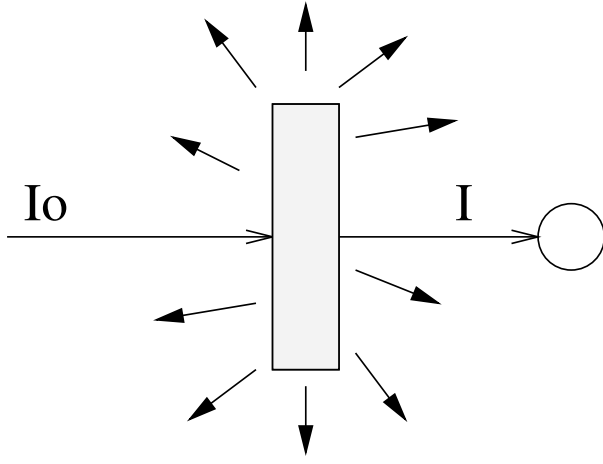
FIG. 13. Schematic diagram of an attenuation measurement.

enceLibrary Stacks.

[3] A. Henry, *Nuclear Reactor Analysis* (MIT Press, Cambridge, MA, 1975) qC786.5.H46 Science Library Stacks.

[4] A. Nero, *Guidebook to Nuclear Reactors* (U.C. Press, Berkeley, CA, 1979) tK9202.N45 Science Library Stacks.

[5] W. H. Bragg and W. L. Bragg, "Analysis of crystal structure by means of x-rays," Nobel Prize Lecture (1915).

[6] C. Kittel and H. Kroemer, *Thermal Physics* (W.H. Freeman, New York, 1980) qC311.5.K62 Physics Department Reading Room.

[7] F. Reif, *Fundamentals of Statistical and Thermal Physics* (McGraw-Hill, New York, 1965) qC175.R361 Physics Department Reading Room.

[8] P. Tipler, *Foundations of Modern Physics* (Worth Publishers, Inc., 1969) qC21.T595 Science Library Stacks.

[9] J. McGervey, *Introduction to Modern Physics* (Academic Press, New York, 1971) qC21.2.M145 Physics Department Reading Room.

[10] B. Rossi, *Optics* (Addison Wesley, Reading, 1957) qC355.R831 Physics Department Reading Room.

[11] "Neutron experimental setup," MIT NSE (2012).

Appendix A: Equipment List

Manufacturer	Description	URL
MIT	Research Reactor	
LND	He-3 Detector	lnd.com
LND	BF$_3$ Detector	lnd.com
Canberra	Proportional Counter preamp	canberra.com
Canberra	Amplifier	canberra.com
Ortec	Multi-Channel Scaler	ortec-online.com

Appendix B: Transmission Cross Section Measurement

As illustrated schematically in Figure 13, one measures the diminution in the beam intensity caused by the insertion of a given absorber between the beam and the detector. The data consist of the total numbers of neutrons detected per unit time, N_0 and N, integrated over the time-of flight spectrum, with correction for background (baseline), and with and without the sample in the monochromatic neutron beam. One then calculates the transmission T and finally the effective cross sectional area s of the scattering-absorption center according to the relation

$$T = \frac{I}{I_0} = \frac{N}{N_0} = e^{-M\sigma}. \tag{B1}$$

Question 1: What is the uncertainty $\Delta\sigma$ in the σ value?

Answer: From the theory of propagating errors we have the equation

$$\left(\frac{\Delta T}{T}\right)^2 = \left(\frac{\Delta N}{N}\right)^2 + \left(\frac{\Delta N_0}{N_0}\right)^2, \tag{B2}$$

i.e. the fractional error in T is the square root of the sum of the squares of the fractional errors in the the intensity values. Since $\Delta N = \sqrt{N}$ for a statistically random collection of N events, it follows that

$$\frac{\Delta T}{T} = -M\Delta\sigma = \left(\frac{1}{N} + \frac{1}{N_0}\right)^{1/2}. \tag{B3}$$

Question 2: If we want to spend a total collection time t_0 distributed between sample collection time t_s and incident beam collection time t_B, what is the optimum distribution of collection time so as to minimize ΔT and $\Delta\sigma$?

Answer: $N_0 = \alpha t_B$ and $N = T\alpha t_s$, where α is the collection rate of incident beam intensity and $t_s = t_0 - t_B$. It follows that

$$\frac{\Delta T}{T} = \left(\frac{1}{T\alpha t_s} + \frac{1}{\alpha t_B}\right)^{1/2}. \tag{B4}$$

For minimization of ΔT, we want

$$\frac{d(\Delta T)}{dt_B} = 0. \tag{B5}$$

This is satisfied when

$$\frac{1}{T(t_0 - t_B)^2} - \frac{1}{t_B^2} = 0, \tag{B6}$$

(check this) which, when solved for t_B, yields the expressions

$$t_B = t_0 \frac{\sqrt{T} - T}{1 - T} \tag{B7}$$

and

$$t_s = t_0 - t_B = t_0 \frac{1}{1 + \sqrt{T}}, \qquad (B8)$$

and the ratio of collection times

$$t_s/t_B = T^{-1/2}. \qquad (B9)$$

Thus for high T (*i.e.* $T \approx 1$) we want equal collection times. On the other hand, for small T, we want to distribute the time so that more time is spent collecting neutrons through the sample. For example, if $T = 0.1$ for a sample, you will attain highest precision in the calculated value for σ if the sample collection time is about three times longer than the open beam collection time. Of course, increasing the total collection time t_0 also improves the precision. In estimating how you should best distribute the collection time, you can get a preliminary estimate of T for a sample by looking at the rate of intensity build-up on the MCS scope and comparing this with that obtained with the open beam.

A good sequence procedure for studying the different samples at fixed $\theta_B = 20°$ position is: (1) open beam, (2) Al, (3) Fe, (4) B, (5) Cd, and (6) open beam. Hopefully your start–end "open beam" results are the same and you can average them. Time all collection runs so that they can be normalized.

In placing samples along the beam line, remember that we do not want to count any of the scattered intensity. This means that we want scattering samples to be well away from the detector so that the detector solid angle as seen from the sample is small compared to total 4π steradians.
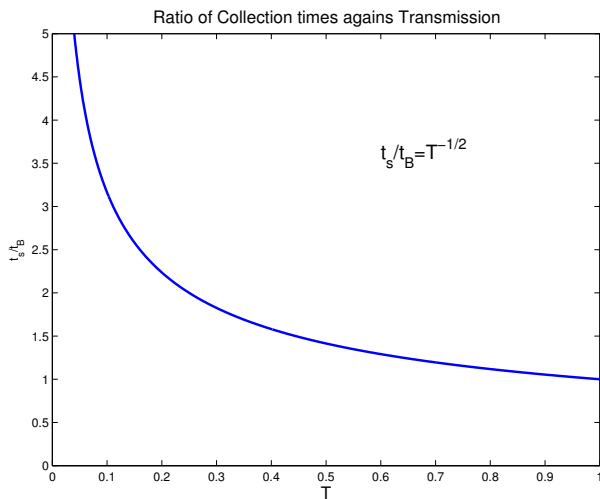

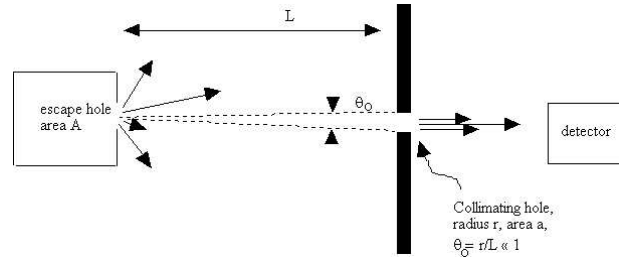FIG. 14. Plot of the ratio of collection times against transmission.

FIG. 15. Schematic of geometry necessary to calculate the neutron flux and neutron density.

Appendix C: Calculation of Neutron Flux and Neutron Density in Reactor

The neutron density n (neutrons/cm^3 irrespective of speed or direction of travel) and the neutron flux $\phi_0 = nv$ (neutrons/cm^2/sec) inside the reactor may be calculated from your intensity measurement obtained in Section IV.1 Item 3. We can model this problem as being similar to that found in many textbooks of statistical mechanics or thermodynamics. (In particular, see Sections 7.9–7.12 in Reference [7]).

Consider a gas of density n in thermal equilibrium inside a container surrounded by vacuum. A small hole is present in the container wall so that gas atoms of all speeds traveling in all directions escape out through the hole.

An additional collimating hole is placed at a large distance L from the container wall along a line perpendicular to the container wall so that a collimated beam of atoms of all speeds will pass through the collimating hole and be detected by a detector placed behind the hole. Thus following Reif Eq. 7.11.9, the collimated current I (atoms/second) passing through the collimating hole would be expressed as

$$
\begin{aligned}
I =& A \int_{v_x > 0} v^3 f(v) dv \int_0^{\theta_0} \sin\theta \cos\theta d\theta \int_0^{2\pi} d\phi \\
=& \pi A \theta_0^2 \int_0^\infty v^3 f(v) dv \\
=& \frac{1}{4} A \theta_0^2 n\bar{v} \\
=& A \frac{a}{4\pi L^2} n\bar{v}, \qquad (C1)
\end{aligned}
$$

where as in Reif, $\bar{v}$ is the average speed of the Maxwell-Boltzmann speed distribution. The average speed is related to our most probable speed v_0 (see Equation 3) as

$$\bar{v} = \frac{2}{\sqrt{\pi}} v_0, \qquad (C2)$$

which you have evaluated in the Maxwell-Boltzmann spectrum analysis.

For our neutron case, neutrons are delivered to a low efficiency detector ($e = 0.010$ averaged over the spectrum) behind the chopper area ($a = 2.4$ mm^2) by a long,

converging, tapered collimator tube. The dimensions of this collimator tube are such that each point of the exit area sees a source area of 2.0 cm^2 on the front surface of the oversize insert tube extending through the D_2O reflector to the center line below the reactor volume. The distance from the exit area (the chopper slit) to the front surface source is 310 cm. Using these numerical parameters and your measured intensity you can calculate $n\bar{v}$ (commonly called the reactor flux) and n. It is to be recognized that these values are approximate (within a small factor of order unity) because our assembly does not match the features of the model exactly. We do not have a sharp containment wall for the neutrons and the void volume of the insert tube can perturb the local flux. This flux value would scale with the reactor operating power level.

Appendix D: Time of Flight Data Analysis

The following analysis was created and provided by Prof. David Litster. *N.b.*: This appendix was written Fall 2010. Components of the experiment (such as the chopper rotation speed, for example) may have been changed since then. Use the information provided here accordingly.

1.   Analysis

This is a brief discussion of how to analyze the TOF data for thermal neutrons.

The flux of neutrons with speeds between v and $v + dv$ will be proportional to

$$j(v)dv = n\sqrt{\frac{2}{\pi}}\left(\frac{v}{v_0}\right)^3 e^{-(v/v_0)^2}dv, \qquad \text{(D1)}$$

where

$$v_0 = \sqrt{2k_B T/m} \approx 2300 \text{ ms}^{-1}. \qquad \text{(D2)}$$

If the detector efficiency is proportional to $1/v$ we might expect a neutron counting rate for neutrons with speeds between v and $v + dv$ to be proportional to

$$\left(\frac{v}{v_0}\right)^2 e^{-(v/v_0)^2}dv \qquad \text{(D3)}$$

However, the chopper passes neutrons for a finite period of time every time it opens. Thus the time of flight of the neutrons from the chopper to the detector varies and the counts in each channel of the MCS represent neutrons that have a range of speeds. When the detector is close to the chopper, that does not matter much as neutrons of all speeds present in the beam will arrive at the detector at the same time (on the scale of the time resolution for the chopper) and the counts in the MCS will just measure the transmission of the chopper as a function of time. That function will be the convolution of two slits each 1.0 mm wide and will therefore be triangular in shape. The chopper wheel spins at 1800 rpm and the slits are at a radius of 54.5 mm. From this, it is easy to calculate that the triangular transmission function of the chopper should have a half-width at the base of 95 μs. This was verified by fitting the TOF spectrum obtained when the BF$_3$ detector was 3.25 in from the chopper. I will use the variable t_H to represent the 95 μs half-width of the chopper transmission. I will also use ℓ to be the distance from the chopper to the BF$_3$ detector and consider the neutrons counted into channel m of the MCS. The sweep of the MCS is triggered by a light pulse some time before the chopper opens. I assume that the MCS is counting into channel n_0 when the chopper transmission is maximum.

Now let's consider channel m of the MCS. It will represent a time $t_m = t_D(m - n_0)$ with respect to the time the chopper was maximally open. Note that t_m may be negative. If $t_m \leq -t_H$ no neutrons will have had time to reach the detector. For $t_m > -t_H$, there are three time regions to consider when calculating the neutron speeds that will be counted into channel m. They are $-t_H < t_m \leq 0$, $0 < t_m \leq t_H$, and $t_m > t_H$.

The easiest way to do the calculations is to consider the travel time t of the neutrons from the chopper to the detector. When integrating over the range of speeds for neutrons that will be counted into channel m, it will be necessary to include a factor that represents the triangular transmission function of the chopper. It will also be useful to introduce a new variable $y = v/v_0 = \ell/(v_o t)$ which means $t = \ell/(v_0 y)$ and $dt = -(\ell/v_0)(1/y^2)dy$.

What we want to integrate over these three time regions is the number of neutrons whose travel time lies between t and $t + dt$. As the number whose speed is between v and $v + dv$ is proportional to $y^2 e^{-y^2}dv$ and $t = \ell/v$, the number whose travel time is between t and $t + dt$ will be proportional to $y^4 e^{-y^2}dt$.

Some useful integrals will be:

$$\int_{y_1}^{y_2} e^{-y^2}dy = \frac{\sqrt{\pi}}{2}[\Phi(y_2) - \Phi(y_1)]$$

$$\text{where } \Phi(x) = \frac{2}{\sqrt{\pi}}\int_0^x e^{-t^2}dt, \qquad \text{(D4)}$$

$$\int_{y_1}^{y_2} ye^{-y^2}dy = -\frac{1}{2}\int_{y_1^2}^{y_2^2} e^{-z}dz = \frac{1}{2}\left(e^{-y_1^2} - e^{-y_2^2}\right),$$

$$\int y^2 e^{-y^2}dy = -\frac{1}{2}ye^{-y^2} + \frac{1}{2}\int e^{-y^2}dy .$$

The calculations are given below. The neutron count rate will be proportional to $\mathcal{R}(m)$ and the factor $1/t_H$ is included to make the result dimensionless.

$-t_H < t_m \leq 0$:

$$\mathcal{R}(m) = \frac{1}{t_H} \int_0^{t_H+t_m} \left(\frac{t_H + t_m - t}{t_H} \right) y(t)^4 e^{-y(t)^2} dt$$

$$= \frac{\ell}{v_0 t_H} \int_{y_1}^{\infty} \left[\left(1 + \frac{t_m}{t_H} \right) y^2 - \frac{\ell}{v_0 t_H} y \right] e^{-y^2} dy \text{ where } y_1 = \frac{\ell}{v_0(t_m + t_H)}$$

$$= \frac{1}{2} \frac{\ell}{v_0 t_H} \left(1 + \frac{t_m}{t_H} \right) \left(\frac{\sqrt{\pi}}{2} [1 - \Phi(y_1)] + y_1 e^{-y_1^2} \right) - \frac{1}{2} \left(\frac{\ell}{v_0 t_H} \right)^2 e^{-y_1^2}$$

$0 < t_m \leq t_H$:

$$\mathcal{R}(m) = \frac{1}{t_H} \int_0^{t_m} \left(\frac{t_H - t_m + t}{t_H} \right) y(t)^4 e^{-y(t)^2} dt + \frac{1}{t_H} \int_{t_m}^{t_H+t_m} \left(\frac{t_H + t_m - t}{t_H} \right) y(t)^4 e^{-y(t)^2} dt$$

$$= \frac{\ell}{v_0 t_H} \int_{y_1}^{y_m} \left[\left(1 + \frac{t_m}{t_H} \right) y^2 - \frac{\ell}{v_0 t_H} y \right] e^{-y^2} dy + \frac{\ell}{v_0 t_H} \int_{y_m}^{\infty} \left[\left(1 - \frac{t_m}{t_H} \right) y^2 + \frac{\ell}{v_0 t_H} y \right] e^{-y^2} dy$$

$$= \frac{1}{2} \frac{\ell}{v_0 t_H} \left\{ \frac{\sqrt{\pi}}{2} [1 - \Phi(y_1)] + y_1 e^{-y_1^2} - \frac{t_m}{t_H} \left[\frac{\sqrt{\pi}}{2} [1 + \Phi(y_1) - 2\Phi(y_m)] + 2y_m e^{-y_m^2} - y_1 e^{-y_1^2} \right] \right\}$$

$$+ \frac{1}{2} \left(\frac{\ell}{v_0 t_H} \right)^2 \left[e^{-y_1^2} - 2e^{-y_m^2} \right] \text{ where } y_m = \frac{\ell}{v_0 t_m} \ .$$

$t_m > t_H$:

$$\mathcal{R}(m) = \frac{1}{t_H} \int_{t_m-t_H}^{t_m} \left(\frac{t_H - t_m + t}{t_H} \right) y(t)^4 e^{-y(t)^2} dt + \frac{1}{t_H} \int_{t_m}^{t_H+t_m} \left(\frac{t_H + t_m - t}{t_H} \right) y(t)^4 e^{-y(t)^2} dt$$

$$= \frac{\ell}{v_0 t_H} \int_{y_1}^{y_m} \left[\left(1 + \frac{t_m}{t_H} \right) y^2 - \frac{\ell}{v_0 t_H} y \right] e^{-y^2} dy + \frac{\ell}{v_0 t_H} \int_{y_m}^{y_2} \left[\left(1 - \frac{t_m}{t_H} \right) y^2 + \frac{\ell}{v_0 t_H} y \right] e^{-y^2} dy$$

$$= \frac{1}{2} \frac{\ell}{v_0 t_H} \left\{ \Gamma(\tfrac{3}{2}, y_1^2) - \Gamma(\tfrac{3}{2}, y_2^2) + \frac{t_m}{t_H} [\Gamma(\tfrac{3}{2}, y_1^2) + \Gamma(\tfrac{3}{2}, y_2^2) - 2\Gamma(\tfrac{3}{2}, y_m^2)] \right\}$$

$$+ \frac{1}{2} \left(\frac{\ell}{v_0 t_H} \right)^2 \left[e^{-y_1^2} + e^{-y_2^2} - 2e^{-y_m^2} \right] \text{ where } y_2 = \frac{\ell}{v_0(t_m - t_H)}.$$

Thus $\mathcal{R}(m)$ has exponentials along with error functions. These should not be too hard to evaluate numerically for fitting purposes. Most compiler libraries provide them. The GNU Scientific Library (http://www.gnu.org/software/gsl/) has routines for both of these functions. The exponential function goes rapidly to zero for large x and can lead to floating point underflows. I used code provided in the GSL library to deal with that.

When writing the fitting code, it is easy to measure time in MCS channel number units and use the dwell time to convert to microseconds after the fit. The model function code that I used is listed below. It is written in C and there are some global variables: NO is n_0, X is the channel number so that $\mathtt{m} = \mathtt{X} - \mathtt{NO}$ is t_m, HW is t_H, $\mathtt{p} = \mathtt{PK} - \mathtt{NO}$ is ℓ/v_0, all expressed in channel number units. The quantities NO, PK, HW, BG, and SF are all the parameters that may be varied in the fit. Once HW and NO have been found from fitting data taken with the detector close to the chopper, they are then held fixed. (The value of HW found from the fit should, of course, agree with the

calculated value from the chopper and slit dimensions and chopper rotation speed.)

My code was written for a nice fitting/plotting package called C-Plot, available from Certified Scientific Software (http://www.certif.com/). You could use it as pseudocode to guide code you write for Matlab or some other package.

2.   Necessity

How necessary is this correction for the finite opening time of the chopper? As you might expect, it depends on how t_H compares to the time for the neutrons to travel to the detector. The graph below shows some calculated fits with $t_H = 25$ channels (close to the 95 μs calculated value for the chopper) and $t_H = 1$ channel, essentially no correction for chopper open time. I used $n_0 = 100$ channels, which is close to correct for the apparatus. The plots are for thermal spectra with $\ell/v_0 = 10$ channels and

$\ell/v_0 = 100$ channels; the latter is about what one expects for $t_D = 4$ μs and thermal neutrons when $\ell = 1$ m.

TOF: effect of t_H
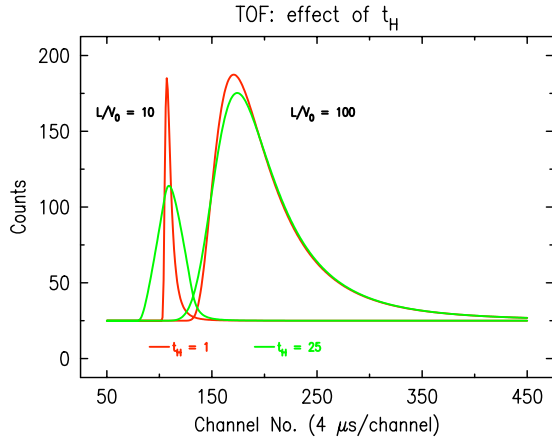
The correction is not important for thermal neutrons at $\ell = 1$ m, but it matters close to the chopper and for the epithermal peak seen in the spectrum at $\ell = 1$ m.

The fast peak above has a speed about 2.5×10^4 m/s, obtained from the peak position shift of about 45 μs as the detector was moved 1.0 m. As the plot shows, a Maxwell-Boltzmann distribution with this v_0 would rise and fall so rapidly that the fit function is essentially the triangular transmission of the chopper. (The same must be true for whatever is the actual speed distribution of the fast neutrons.) This v_0 would correspond to a thermal distribution for $T \approx 3 \times 10^4$ K. The epithermal neutrons are moving so fast and their speed distribution is sufficiently narrow that even after they have traveled 1 m we cannot determine it with a chopper whose time resolution is given by $t_H \approx 100$ μs. However it is very unlikely to be thermal.

Fits of the thermal functions to my data are shown on the next page; the fits and plots were made with C-PLOT.

TOF at Z = 3.25
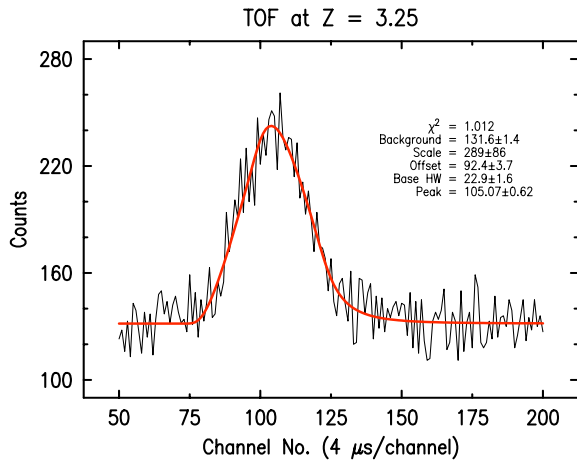
After 1 m, the scan appears to separate into two peaks. Each was fit individually to a thermal spectrum. One seems to have v_0 about 12 times the other.

Total TOF at Z = 42.62
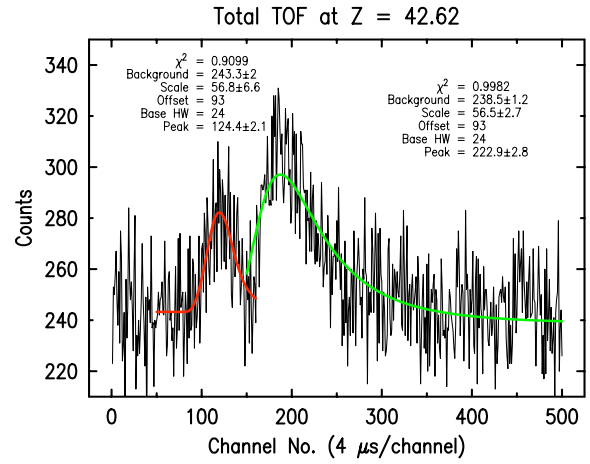
Finally, the fit obtained to the fast peak portion of the scan was subtracted (with zero background) from the total data. This should, in principle, leave only the background and the neutron counts from the slow (thermal) neutrons. The data that resulted are shown in the plot below along with the fit to all of the data.

Slow Peak TOF at Z = 42.62
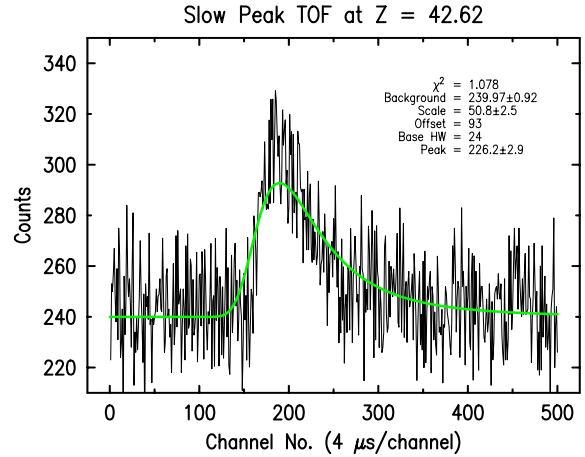
The result agrees with that obtained only by fitting data in channels above number 150. The value of v_0 obtained from the fit is about 2000 m/s. The value obtained using the peak shift from $Z = 3.25$ to $Z = 42.62$ ($\Delta\ell = 1.00$ m) would be 2100 m/s. The fast peak shift suggests a speed about 13000 m/s, while the average speed obtained from the fit of the $Z = 3.25$ data to a thermal spectrum (unreliable, in my view) would be $v_0 \simeq 20000$ m/s.

This suggests to me that 93 is too low for the offset channel number and a better value would be somewhere from 95 to 100. If the angle the chopper wheel has to rotate after the light pulse until the first slit is fully open were to be measured, then the offset channel number n_0 could be calculated.

3. C-Plot code

Below is the C-PLOT model function code used to perform the analysis described in Section 1.

```
#define RP 0.88622693          /* \sqrt{\pi}/2 */

double  model(deriv_flag)
int        deriv_flag;
{
  double m, p, yfit;
  double y1, y2, ym, r;
  double ey1, ey2, eym;       /* exponentials */
  double py1, py2, pym;       /* error functions */

  m = X - NO;
  p = PK - NO;
  if (p < 1.0) p = 1.0;
  if (m <= (-HW)) {
    r = 0;
  }
  else if (m <= 0) {
     y1 = p/(m+HW);
     py1 = gs1_sf_erf(y1);
     status = gsl_sf_exp_e(y1*y1, &result);
     if (status) {
        ey1 = 0.0;
        if (status != GSL_EUNDRFLW)
        printf("exp(-y1*y1) m=%g %s\n", m, gsl_strerror(status));
     }
     else ey1 = result.val;
     r = (p/HW)*( RP*(1.0 - py1) + y1*ey1
       + (m/HW)*( RP*(1.0 - py1) + y1*ey1 ) - (p/HW)*ey1 );
   }
   else if (m <= HW) {
     y1 = p/(m+HW);
     py1 = gsl_sf_erf(y1);
     status = gsl_sf_exp_e(y1*y1, &result);
     if (status) {
        ey1 = 0.0;
        if (status != GSL_EUNDRFLW)
        printf("exp(-y1*y1) m=%g %s\n", m, gsl_strerror(status));
     }
     ym = p/m;
     pym = gsl_sf_erf(ym);
     status = gsl_sf_exp_e(ym*ym, &result);
     if (status) {
        eym = 0.0;
        if (status != GSL_EUNDRFLW)
        printf("exp(-ym*ym) m=%g %s\n", m, gsl_strerror(status));
     }
     else eym = result.val;
     r = (p/HW)*( RP*(1.0 - py1) + y1*ey1
       + (m/HW)*( RP*(2.0*pym - py1 - 1.0) - 2.0*ym*eym + y1*ey1 )
       + (p/HW)*(2.0*eym - ey1) );
   }
   else { /* m > HW */
     y1 = p/(m+HW);
     py1 = gsl_sf_erf(y1);
     status = gsl_sf_exp_e(y1*y1, &result);
     if (status) {
        ey1 = 0.0;
        if (status != GSL_EUNDRFLW)
        printf("exp(-y1*y1) m=%g %s\n", m, gsl_strerror(status));
     }
     else ey1 = result.val;
     ym = p/m;
     pym = gsl_sf_erf(ym);
     status = gsl_sf_exp_e(ym*ym, &result);
     if (status) {
        eym = 0.0;
        if (status != GSL_EUNDRFLW)
        printf("exp(-ym*ym) m=%g %s\n", m, gsl_strerror(status));
     }
     else eym = result.val;
     y2 = p/(m-HW);
     py2 = gsl_sf_erf(y2);
     status = gsl_sf_exp_e(y2*y2, &result);
     if (status) {
        ey2 = 0.0;
        if (status != GSL_EUNDRFLW)
        printf("exp(-y2*y2) m=%g %s\n", m, gsl_strerror(status));
     }
     else ey2 = result.val;
     r = (p/HW)*( RP*((py2 - py1) + y1*ey1 - y2*ey2
       + (m/HW)*( RP*(2.0*pym - py1 - py2)) - 2.0*ym*eym + y1*ey1
       + (p/HW)*(2.0*eym - ey1 - ey2) );
   }
  yfit = BG +SF * r;
  if (deriv_flag) {
     if (fBG) dBG = 1;
     if (fSF) dSF = r;
  }
  return(yfit);
}
```